RESEARCH PAPER

Development and Characterization of Chitosan Based Simvastatin and PDGF Loaded Novel Delivery System for Treatment of Wound

Bhaskar Kumar Gupta[1], Surendra Dangi[2]*
[1, 2] School of Pharmacy and Research, People's University, Bhopal, Madhya Pradesh, India.
Corresponding author: Surendra Dangi, *Email:* dangipip@gmail.com

Abstract
Diabetic wounds represent a formidable clinical challenge characterized by chronic inflammation, severe oxidative stress, and diminished endogenous growth factors, which collectively stall the physiological healing cascade. To overcome these multifactorial barriers, this study developed a multi-targeted, "smart" topical drug delivery system integrating simvastatin-loaded nanoparticles and Platelet-Derived Growth Factor (PDGF) within a bio-responsive ointment. Simvastatin and L-Arginine/Silver nanoparticles were synthesized via a modified solvent emulsification-evaporation technique and statistically optimized using a Box-Behnken Design, achieving a refined mean particle size of 141.5 nm and an entrapment efficiency of 66.60%. These optimized nanocarriers and exogenous PDGF were successfully embedded into a degradable, glutaraldehyde-crosslinked chitosan-gelatin water-in-oil ointment (SAPNP). *In vitro* evaluations demonstrated that the SAPNP matrix provided sustained, biphasic drug release governed by first-order kinetics, potent antioxidant and antibacterial activity, and exceptional biocompatibility, actively stimulating NIH/3T3 fibroblast proliferation up to 116.71%. The therapeutic efficacy was evaluated *in vivo* utilizing a streptozotocin (STZ)-induced diabetic rat excisional wound model. The SAPNP formulation dramatically accelerated macroscopic wound contraction, achieving complete and mature re-epithelialization in 17 days, compared to 29 days for the diabetic control. Biochemical and histopathological analyses confirmed that the synergistic treatment restored localized oxidative balance by elevating Superoxide Dismutase (SOD) and Catalase, doubled total cellular protein, and significantly upregulated structural collagen (hydroxyproline) and glycosaminoglycans (hexosamine). The combinational delivery of pleiotropic simvastatin nanocarriers and mitogenic PDGF within a biomimetic scaffold successfully overrides the hostile diabetic microenvironment, offering a highly effective, advanced therapeutic platform for chronic wound regeneration.

Keywords: Diabetic wound healing; Simvastatin-loaded nanoparticles; L-Arginine; Silver nanoparticles; Platelet-Derived Growth Factor (PDGF); Chitosan–gelatin ointment; Box–Behnken Design; Antioxidant activity; Re-epithelialization; Tissue regeneration.
How to cite this article: Bhaskar Kumar Gupta1 Surendra Dangi2*. Development and Characterization of Chitosan Based Simvastatin and PDGF Loaded Novel Delivery System for Treatment of Wound. Int J Drug Deliv Technol. 2026;16(90s):1049-1060. DOI: 10.25258/ijddt.16.90s.102.

Introduction

Diabetes mellitus is a chronic metabolic disorder affecting millions worldwide, with India having a particularly high disease burden. Approximately 20% of diabetic patients develop chronic, non-healing wounds, particularly diabetic foot ulcers, which may lead to serious complications and amputations. Unlike normal wound healing, which involves hemostasis, inflammation, proliferation, and tissue remodeling, diabetic wounds remain in a prolonged inflammatory state due to impaired glucose metabolism, delayed tissue regeneration, and reduced collagen formation. Chronic hyperglycemia increases reactive oxygen species (ROS), causing oxidative stress, impaired nitric oxide (NO) production, reduced angiogenesis, and poor blood circulation. Additionally, decreased growth factors, particularly Platelet-Derived Growth Factor (PDGF), and excessive matrix metalloproteinase (MMP) activity accelerate extracellular matrix degradation. Impaired immune responses further increase the risk of persistent bacterial infections.

Conventional wound management approaches are often insufficient to address these complex pathological changes, highlighting the need for advanced multifunctional drug delivery systems. The present study proposes a novel topical ointment incorporating a chitosan–gelatin biopolymer matrix containing simvastatin-loaded L-arginine/silver nanoparticles (SANP) and PDGF. Simvastatin provides anti-inflammatory, antioxidant, and pro-angiogenic effects, while L-arginine supports nitric oxide production and silver nanoparticles offer antimicrobial activity. Additionally, PDGF promotes fibroblast proliferation, cell migration, and collagen deposition. Thus, the proposed simvastatin- and PDGF-loaded biopolymer ointment (SAPNP) aims to provide a multifunctional therapeutic approach for improving wound healing, reducing infection, and promoting tissue regeneration in diabetic wounds.

Materials and Methods

Materials

Simvastatin and PDGF were procured from Life Technologies (India). Chitosan, gelatin, L-arginine, silver nitrate, solvents, 4-hydroxy-L-proline, and glucosamine hydrochloride were obtained from HiMedia Laboratories. MMP primers, TRIzol

reagent, reverse transcription master mix, and ELISA kits were purchased from Invitrogen. Streptozotocin and superoxide dismutase were obtained from Merck and Sigma-Aldrich, respectively. Ultrapure water was prepared using a Milli-Q purification system. All chemicals were of analytical grade.

Preparation and Optimization of Nanoparticles

Synthesis: Plain arginine nanoparticles (ANPs) and simvastatin-loaded nanoparticles (SNPs) were prepared using a modified solvent emulsification–evaporation technique. Statistical Optimization: Formulations were optimized using a 17-run, three-factor Box–Behnken Design (BBD) in Design-Expert software, evaluating polymer concentration, aqueous-to-organic phase ratio, and surfactant concentration against particle size and entrapment efficiency.

Characterization of Nanoparticles

Physicochemical Evaluation: Particle size, PDI, and zeta potential were measured using a Malvern Zetasizer Nano ZS 90, while morphology was examined by TEM.

Encapsulation and Characterization: Entrapment efficiency (%EE) and drug loading (%DL) were determined using UV-Vis spectroscopy at 238 nm. DSC was used for solid-state characterization.

In Vitro Release and Stability: Drug release was studied using a modified Franz diffusion cell and fitted to standard kinetic models. Stability was evaluated for 180 days according to ICH Q1A(R2) guidelines

In Vitro Characterization of Ointment Formulations

Physical Evaluation: Ointments were evaluated for homogeneity, pH, viscosity, spreadability, extrudability, swelling, and moisture permeability.

In Vitro Drug Release: Simvastatin and PDGF release were studied using phosphate buffer (pH 7.4) with 0.5% sodium lauryl sulfate, followed by kinetic modeling.

Antioxidant and Antibacterial Activity: Antioxidant activity was assessed using DPPH and NBT assays, while antibacterial activity against Pseudomonas aeruginosa was evaluated by agar well diffusion.

Cell Viability: Cytotoxicity and biocompatibility were assessed using the MTT assay in NIH/3T3 fibroblast cells.

In Vivo Wound Healing Studies

Animal Model: The study was approved by IAEC (Approval No. PBRI/IAEC/21-04-2026/026) and conducted according to CCSEA guidelines. Diabetes was induced in Wistar rats (120–150 g) using streptozotocin (65 mg/kg, i.p.).

Wound Creation and Treatment: Full-thickness excisional wounds (100 mm^2) were created on the dorsal region and treated with vehicle control, Cipladine, SNP, SANP, or SAPNP ointments.

Wound Healing Assessment: Healing was evaluated through percentage wound contraction and epithelialization period.

Biochemical and Histopathological Evaluation: Granulation tissue was analyzed for total protein, SOD, catalase, hydroxyproline, and hexosamine. H&E-stained tissue sections were examined for ECM remodeling, cellular infiltration, and angiogenesis.

Procedure

The formulations were developed as water-in-oil (w/o) emulsions containing a chitosan–gelatin biopolymer matrix (CGB) and active nanoparticles in the internal aqueous phase. Hydrophobic simvastatin was micro-dispersed, while PDGF was incorporated under cold conditions to preserve its bioactivity.

Procedure for Simvastatin Nanoparticle (SNP) Ointment

- **Step 1: Preparation of Nanoparticles (Phase A):** Dissolve 0.05 g of Silver Nitrate ($AgNO_3$) in 5.0 g of Ultrapure Water. Add 0.25 g of L-Arginine and stir under moderate heat (approximately 60°C) until a color change to a light brown or yellowish hue occurs, indicating silver nanoparticle formation. Set aside to cool.
- **Step 2: Preparation of the Biopolymer Hydrogel (Phase B):** Mix 20.0 g of Ultrapure Water with 1.00 g of Glacial Acetic Acid. Gradually sprinkle 1.50 g of Medium MW Chitosan into the acidic water under continuous magnetic stirring until a clear, viscous solution forms. Heat gently to 40-45°C and slowly disperse 3.00 g of Gelatin, stirring until fully hydrated and uniform.
- **Step 3: Preparation of the API (Phase C):** Dissolve 1.20 g of Simvastatin in a solvent mixture of 4.00 g Dichloromethane (DCM) and 1.00 g Methanol within a fume hood.
- **Step 4: Integration of API and Nanoparticles:** Add the Simvastatin solution (Phase C) dropwise into the stirring Biopolymer hydrogel (Phase B). Introduce the cooled Silver Nanoparticle solution (Phase A) and homogenize. Volatile solvents evaporate during this step, facilitating simvastatin entrapment.
- **Step 5: Preparation of Ointment Base (Phase D):** Melt 58.00 g of Degradable Oil Base and 5.00 g of Lipophilic Surfactant in a water bath at 50-55°C until uniform.
- **Step 6: Final Emulsification:** Ensure both the combined aqueous phase and the lipid base are at 45-50°C. Slowly pour the aqueous mixture into the lipid base under high-shear homogenization for 10-15 minutes to form a smooth w/o emulsion. Cool to room temperature under gentle stirring and package.

Procedure for Simvastatin Arginine Silver Nanoparticle (SANP) Ointment

- **Step 1 (Phase A):** Dissolve 0.10 g $AgNO_3$ in 5.0 g water, add 0.50 g L-Arginine, and stir at 60°C until yellowish-brown.
- **Step 2 (Phase B):** Mix 19.90 g water with 1.00 g Glacial Acetic Acid. Disperse 2.00 g Chitosan, warm to 40-45°C, and hydrate 2.50 g Gelatin.
- **Step 3 (Phase C):** Dissolve 1.00 g Simvastatin in 4.00 g DCM and 1.00 g Methanol.
- **Step 4:** Integrate Phase C and Phase A into Phase B and homogenize.
- **Step 5 & Final Emulsification:** Melt 58.00 g Oil Base and 5.00 g Surfactant at 50-55°C. Combine with the 45-50°C aqueous phase under high-shear homogenization for 10-15 minutes. Cool to room temperature.

Procedure for Composite (SAPNP) Ointment

- **Step 1 (Phase A):** Dissolve 0.10 g $AgNO_3$ in 5.0 g water, add 0.50 g L-Arginine, and heat to 60°C to reduce silver nanoparticles, then cool to room temperature.
- **Step 2 (Phase B):** Mix 19.85 g water and 1.00 g Glacial Acetic Acid. Disperse 1.50 g Chitosan, warm to 40-45°C, and hydrate 3.00 g Gelatin.
- **Step 3 (Phase C):** Dissolve 1.00 g Simvastatin in 4.00 g DCM and 1.00 g Methanol.
- **Step 4:** Incorporate Phase C and Phase A into Phase B and homogenize.
- **Step 5 & Emulsification:** Melt 58.00 g Oil Base and 5.00 g Surfactant at 50-55°C. Emulsify with the aqueous phase (at 45-50°C) under high-shear homogenization for 10-15 minutes, then switch to gentle mechanical stirring to cool.
- **Step 6: Incorporation of Biologics (Phase E):** Once the ointment base cools below 35°C to prevent thermal degradation, carefully fold in 0.05 g of Platelet-Derived Growth Factor (PDGF) using a low-shear mixing method to ensure even distribution. Package in airtight, light-resistant containers.

Results and Discussions

Optimization and Characterization of Nanoparticles

Box–Behnken Design was used to optimize SNPs based on polymer concentration, phase ratio, and surfactant concentration. The optimized SNPs showed a particle size of 141.3 ± 4.2 nm, PDI of 0.235, and entrapment efficiency of 66.60 ± 2.02%, compared with 172.4 ± 8.4 nm for plain arginine nanoparticles. Zeta potential values of −28.85 mV and −31.27 mV indicated good colloidal stability. TEM confirmed spherical nanoparticles with smooth surfaces. DSC analysis indicated the conversion of crystalline simvastatin into an amorphous, encapsulated form. In vitro release showed an initial burst of approximately 25% within one hour, followed by sustained release of 89.99% over 24 hours. Release kinetics followed the Higuchi model, suggesting diffusion-controlled drug release. The formulations remained stable during six months of stability testing.

Table 1: Box-Behnken design of SNPs and their experimental results

Formulation Code	X_1	X_2	X_3	X_1 (Actual)	X_2 (Actual)	X_3 (Actual)	Y_1 (PS, nm)	Y_2 (%EE)	PDI	ZP (mV)
F1	-1	0	1	0.1	2:1	1.5	286.9	60.66	0.420	-26.6
F2	0	-1	-1	0.3	1:1	0.5	221.7	46.6	0.819	-23.4
F3	0	0	0	0.3	2:1	1.0	219.9	71.8	0.398	-17.6
F4	0	0	0	0.3	2:1	1.0	219.9	71.8	0.398	-17.6
F5	-1	0	-1	0.1	2:1	0.5	301.6	29.3	0.447	-26.6
F6	0	0	0	0.3	2:1	1.0	219.9	71.8	0.398	-17.6
F7	0	1	1	0.3	4:1	1.5	107.2	66.9	1.000	-26.2
F8	1	0	1	0.5	2:1	1.5	326.4	60.66	0.480	-13.0
F9	-1	1	0	0.1	4:1	1.0	210.6	46.0	0.664	-22.0

Formulation Code	X_1	X_2	X_3	X_1 (Actual)	X_2 (Actual)	X_3 (Actual)	Y_1 (PS, nm)	Y_2 (%EE)	PDI	ZP (mV)
F10	0	0	0	0.3	2:1	1.0	219.9	71.8	0.398	-17.6
F11	1	-1	0	0.5	1:1	1.0	276.0	40.0	0.474	-19.3
F12	0	-1	1	0.3	1:1	1.5	263.7	66.6	0.481	-24.8
F13	-1	-1	0	0.1	1:1	1.0	342.2	36.0	0.276	-0.23
F14	1	0	-1	0.5	2:1	0.5	364.8	60.6	0.483	-21.9
F15	1	1	0	0.5	4:1	1.0	289.6	61.4	0.626	-23.1
F16	0	1	-1	0.3	4:1	0.5	246.3	64.46	0.660	-19.9
F17	0	0	0	0.3	2:1	1.0	219.9	71.8	0.398	-17.6

Note: Constraints applied were to minimize Y_1 (Particle Size) and maximize Y_2 (Entrapment Efficiency). X_1 = Polymer Concentration (w/v), X_2 = Aqueous/Organic Phase ratio, and X_3 = Surfactant concentration (w/v), where (-1), (0), and (+1) indicate low, medium, and high levels, respectively. ZP = Zeta Potential, PDI = Polydispersity Index.

Table 2: ANOVA for Response Surface Quadratic Model

Source	Y_1 Sum of Squares	Y_1 df	Y_1 Mean Square	Y_1 F-value	Y_1 p-value	Y_2 Sum of Squares	Y_2 df	Y_2 Mean Square	Y_2 F-value	Y_2 p-value
Model	57396.35	9	6377.38	36.63	0.0001*	3083.95	9	332.66	29.17	<0.0001*
X_1	1396.56	1	1396.56	8.02	<0.0253*	218.30	1	218.30	18.60	<0.0035*
X_2	7750.12	1	7750.12	33.53	0.0003*	207.57	1	207.57	17.67	<0.0030*
X_3	2388.65	1	2388.65	13.30	<0.0069*	132.38	1	132.38	12.12	<0.0102*
X_1X_2	5350.92	1	5350.92	30.75	<0.0009*	27.03	1	27.03	2.30	0.1730
X_1X_3	30.96	1	30.96	0.23	0.6323	112.36	1	112.36	9.57	<0.0175*
X_2X_3	8199.30	1	8199.30	37.11	<0.0002*	218.30	1	218.30	18.59	<0.0035*
X_1^2	29303.13	1	29303.13	168.38	0.0001*	160.208	1	160.208	13.630	<0.0001*
X_2^2	2325.26	1	2325.26	13.	<0.00	188.	1	188.	16.	<0.00

Source	Y_1 Sum of Squares	Y_1 df	Y_1 Mean Square	Y_1 F-value	Y_1 p-value	Y_2 Sum of Squares	Y_2 df	Y_2 Mean Square	Y_2 F-value	Y_2 p-value
				93	73*	66		66	06	51*
X_3^2	803.76	1	803.76	3.62	<0.0686	207.32	1	207.32	17.66	<0.0030*
Residual	1218.28	7	173.03			82.22	7	11.75		
Lack of fit	1218.28	3	306.09			82.22	3	27.31		
Pure error	0.0000	3	0.0000			0.0000	3	0.0000		
Cor Total	58613.73	16				3166.17	16			

Note: The Model F-values of 36.64 and 29.17 imply the models are significant. There is only a 0.01% chance that an F-value this large could occur due to noise. * Indicates significance at $p < 0.05$.

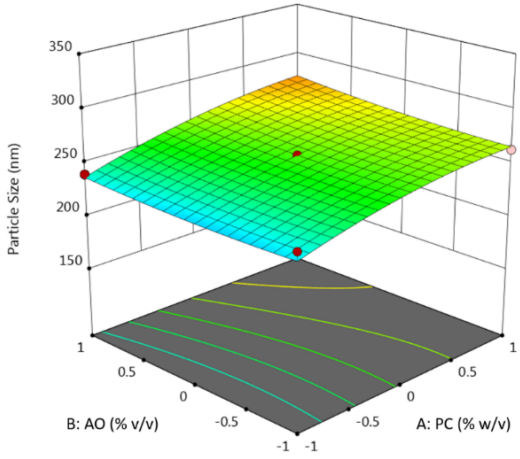

Figure 1: 3D response surface plot for effect of PC – AO interaction terms on particle size

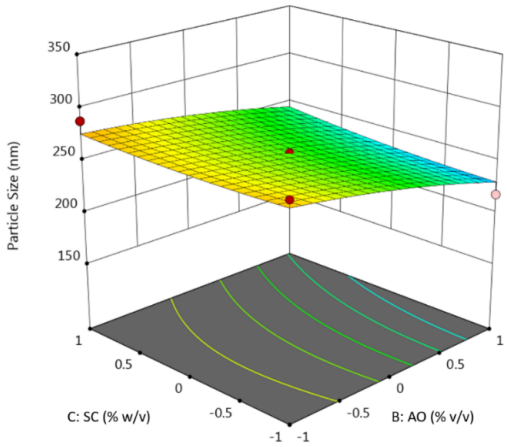

Figure 2: 3D response surface plot for effect of AO-SC interaction terms on particle size

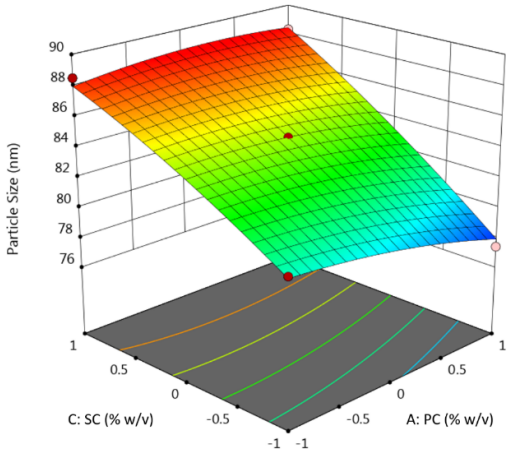

Figure 3: 3D response surface plot for effect of SC –PC interaction terms on particle size

Table 3: Solutions generated by Design-Expert software

Number	Coded X_1 (PC)	Coded X_2 (AO)	Coded X_3 (SC)	Predicted PS (nm)	Predicted EE (%)	Observed EE (%)	Observed PS (nm)	Desirability
1	-0.0043	1.0000	0.4288	138.463	67.285	66.60	141.5	0.885
2	-0.0047	1.0000	0.4335	137.924	67.189	65.00	169.8	0.884
3	-0.0042	1.0000	0.4188	139.014	67.380	62.10	196.7	0.884
4	-0.0070	1.0000	0.4776	134.979	66.631	58.13	195.5	0.883
5	-0.0024	0.9889	0.4644	138.570	67.208			0.883
6	-0.1557	1.0000	0.3331	139.884	66.948			0.877

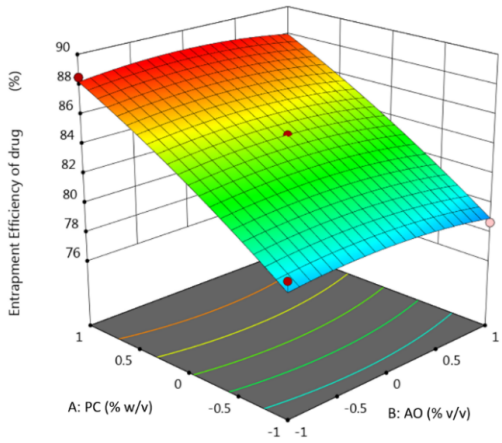

Figure 4: 3D response surface plot for effect of PC – AO interaction terms on entrapment efficiency

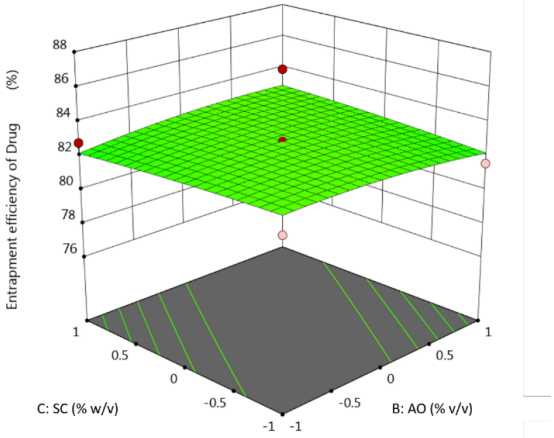

Figure 5: 3D response surface plot for effect of AO – SC interaction terms on entrapment efficiency

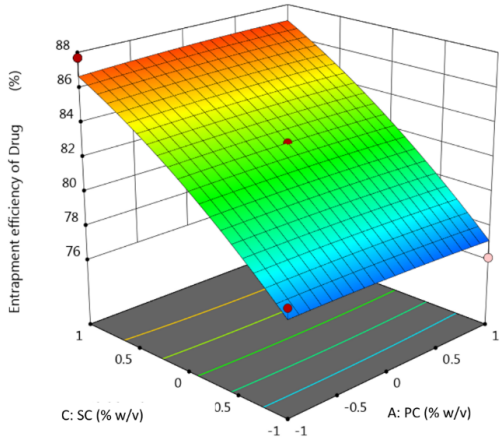

Figure 6: 3D response surface plot for effect of PC – SC interaction terms on entrapment efficiency

Results

		Size (d.nm):	% Intensity:	St Dev (d.n...
Z-Average (d.nm): 172.4	Peak 1:	178.6	95.9	8.4
PdI: 0.459	Peak 2:	0.000	0.0	0.000
Intercept: 0.924	Peak 3:	0.000	0.0	0.000
Result quality : Good				

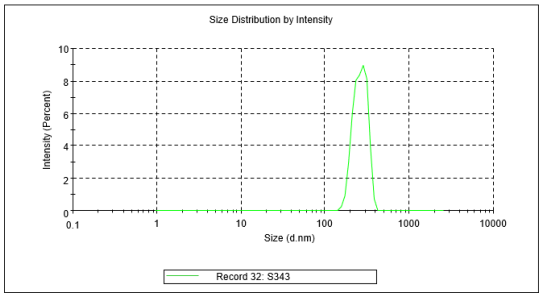

Figure 7: Particle size and PDI of ANPs

Results

		Size (d.nm):	% Intensity:	St Dev (d.n...
Z-Average (d.nm): 141.3	Peak 1:	146.6	80.9	4.2
PdI: 0.235	Peak 2:	0.000	0.0	0.000
Intercept: 0.826	Peak 3:	0.000	0.0	0.000
Result quality : Good				

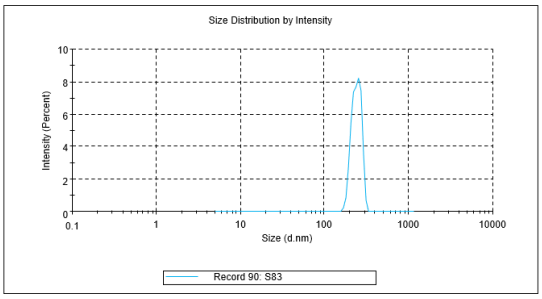

Figure 8: Particle size and PDI of optimized SNPs

Zeta Potential (ZP)

The zeta potential (ZP) of the plain ANPs and the optimized SNPs was determined to be -31.27 ± 2.85 mV and -28.85 ± 1.27 mV, respectively (Figure 9 and Figure 10). These robust ZP values signify that both formulations possess excellent colloidal stability. A high absolute zeta potential (whether negative or positive, typically > ±25 mV) indicates a highly stable nanoparticle dispersion, as the substantial surface charge induces strong electrostatic repulsion between adjacent particles, effectively preventing localized aggregation and coagulation (Lason, 2013).

Results

		Mean (mV)	Area (%)	St Dev (mV)
Zeta Potential (mV): -31.27	Peak 1:	-31.27	100.0	2.85
Zeta Deviation (mV): 2.85	Peak 2:	0.00	0.0	0.00
Conductivity (mS/cm): 10.7	Peak 3:	0.00	0.0	0.00
Result quality : Good				

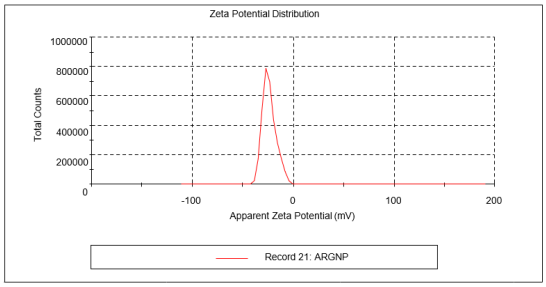

Figure 9: Zeta potential of ANPs

Results

		Mean (mV)	Area (%)	St Dev (mV)
Zeta Potential (mV): -28.85	Peak 1:	-28.85	100.0	1.27
Zeta Deviation (mV): 1.27	Peak 2:	0.00	0.0	0.00
Conductivity (mS/cm): 10.3	Peak 3:	0.00	0.0	0.00
Result quality : Good				

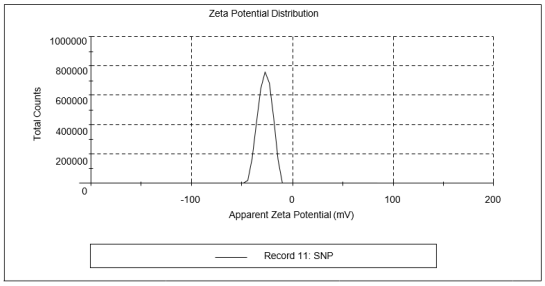

Figure 10: Zeta Potential of optimized SNPs

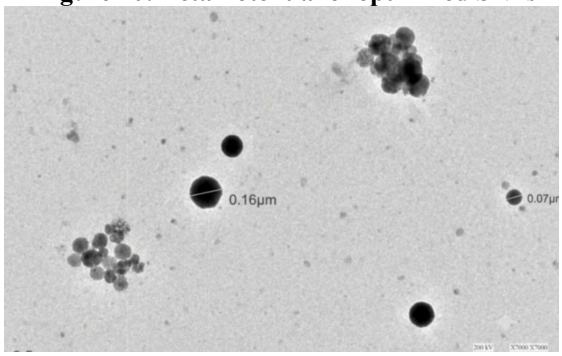

Figure 11: TEM image of plain arginine nanoparticles

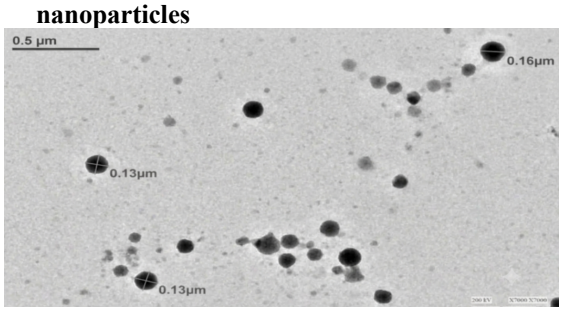

Figure 12: TEM image of Simvastatin loaded nanoparticles

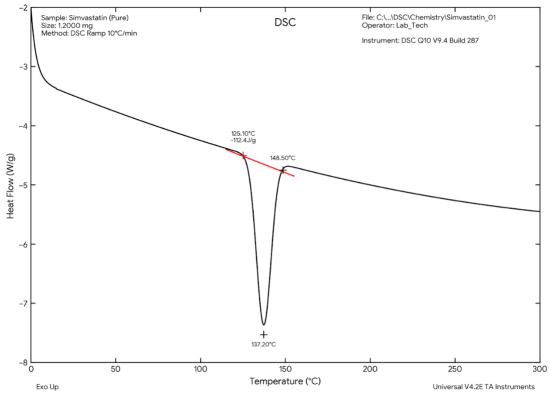

Figure 13: DSC thermogram of Simvastatin

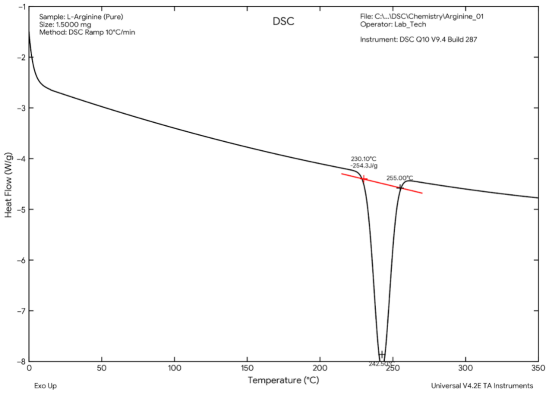

Figure 14: DSC thermogram of L-Arginine

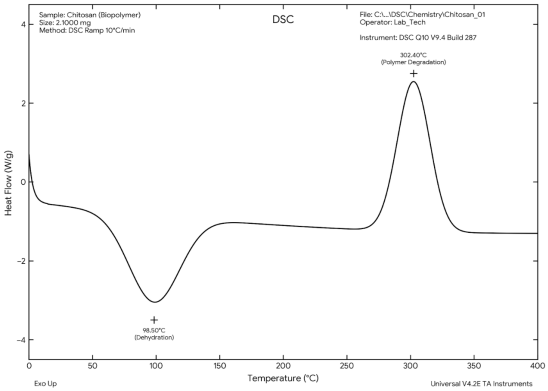

Figure 15: DSC thermogram of Chitosan

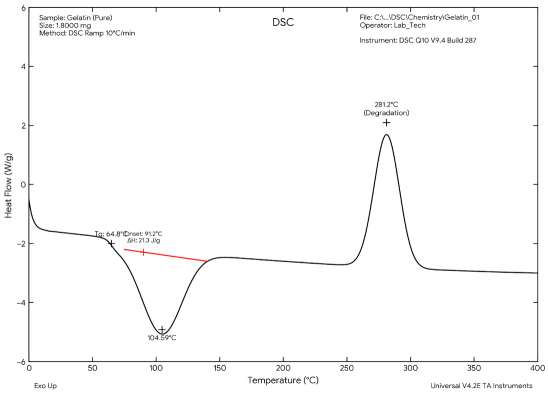

Figure 16: DSC thermogram of Gelatin

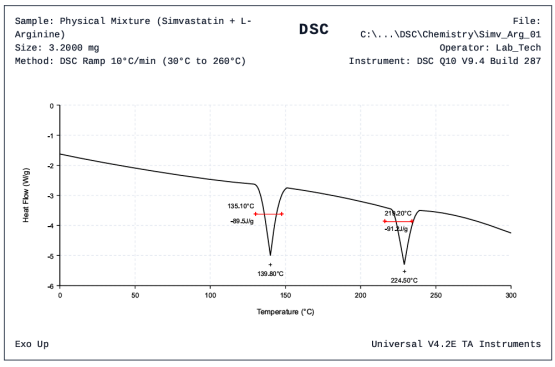

Figure 17: DSC thermograms of Physical mixture of Simvastatin and Arginine

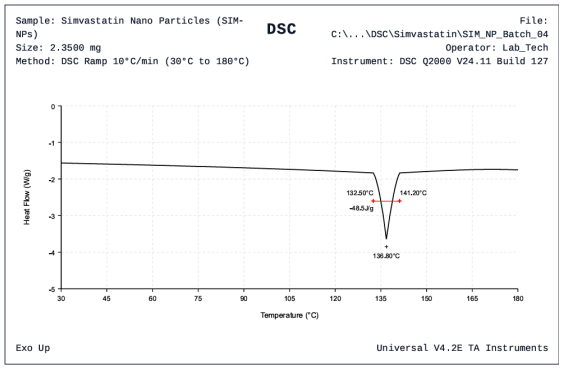

Figure 18: DSC thermograms of SNPs

Physical Characteristics and In Vitro Efficacy of Ointments

The nanoparticles were incorporated into a chitosan–gelatin biopolymer matrix, with formulation F-3 showing optimal flexibility, uniformity, and structural integrity through glutaraldehyde crosslinking. The SNP, SANP, and SAPNP ointments exhibited skin-compatible pH values of 5.9–6.1. In vitro drug release followed first-order kinetics, indicating controlled release through diffusion and matrix swelling. The formulations demonstrated significant antioxidant activity in DPPH and NBT assays and sustained antibacterial activity against Pseudomonas aeruginosa. MTT assays using NIH/3T3 fibroblasts confirmed good biocompatibility, with maximum cell viability of 116.71%. Furthermore, SANP and SAPNP formulations maintained superior physical and chemical stability over 180 days.

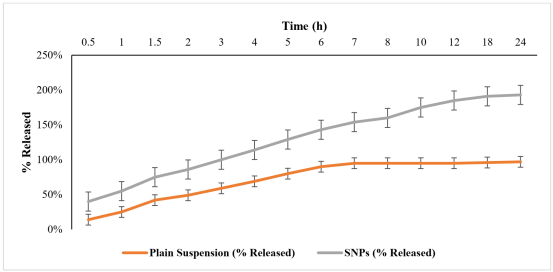

Figure 19: Cumulative drug release of SIM from suspension and SNPs

Table 4: Release behavior of Simvastatin from optimized SIMNPs formulation

Formulation	Zero order	First order		Higuchi		Ritger-Peppas		Hixson Crowell	
	R^2	K	R^2	K	R^2	n	R^2	K	R^2
Optimized SNPs	0.9669	-0.0407	0.97445	15.544	0.99336	0.38	0.93299	-0.889	0.998
Plain Sus	0.9313	-0.1	0.998	41.	0.998	0.7	0.998	-0.	0.999

pension		676	48	32	69	13	86	39	52

Table 5: Results of stability study of SNPs

Formulation	Parameters	Initial Value	1 month		3 months		6 months	
Conditions		(40 ±2º C, 75 ±5 % RH)	(30 ±2 ºC, 65 ±5 % RH)	(40 ±2º C, 75 ±5 % RH)	(30 ±2 ºC, 65 ±5 % RH)	(40 ±2º C, 75 ±5 % RH)	(30 ±2 ºC, 65 ±5 % RH)	(40 ±2 ºC, 75 ±5 % RH)
SIMNPs	PS (nm)	141.5 ± 1.18	142.6 ± 1.02	141.8 ± 1.10	156.6 ± 1.08	153.5 ± 2.02	161.3 ± 1.12	158.6 ± 1.10
	%EE	66.60 ±2.02	65.96 ±1.92	66.90 ±1.82	64.83 ±2.12	64.69 ± 2.34	64.45 ±1.92	65.90 ±1.02
	ZP (mV)	25.90 ±0.28	22.90 ±0.21	25.20 ±0.32	21.30 ±0.40	23.71 ±0.26	19.90 ±0.15	21.60 ±0.22
	PDI	0.256 ±0.22	0.351 ±0.20	0.259 ±0.19	0.526 ±0.21	0.456 ±0.22	0.652 ±0.25	0.446 ±0.29

Table 6: Absorbance and % antioxidant activity of different reaction mixture in DPPH assay & NBT assay

		DPPH Assay						NBT Assay					
	Conc. (µg/mL)	500µg/mL	50µg/mL	25µg/mL	5µg/mL			500µg/mL	50µg/mL	25µg/mL	5µg/mL		
Simvastatin (Pure)	Absorbance	0.020	0.033	0.044	0.065			0.019	0.030	0.044	0.062		
	%AA	94.43	90.59	86.77	81.18			95.02	92	84.5	82.08		
SNP	Time (H)	1h	2h	3h	4h	5h	6h	1h	2h	3h	4h	5h	6h
	Absorbance	0.070	0.065	0.063	0.045	0.05	0.033	0.099	0.088	0.065	0.050	0.039	0.030
	%AA	79.83	81.29	81.82	87.06	88.21	90.62	66.21	70.10	77.10	83.11	86.90	90.01
SANP	Time (H)	1h	2h	4h	8h	12h	16h	1h	2h	4h	8h	12h	16h
	Absorbance	0.097	0.088	0.077	0.070	0.066	0.053	0.12	0.92	0.089	0.078	0.070	0.054

	%AA	62.03	68.24	72.03	76.05	79.70	83.10	58.10	64.05	65.35	69.25	75.2	81.5
SAPNP	**Time (H)**	**1h**	**2h**	**4h**	**8h**	**12h**	**16h**	**1h**	**2h**	**4h**	**8h**	**12h**	**16h**
	Absorbance	0.099	0.092	0.080	0.068	0.062	0.050	0.098	0.94	0.090	0.077	0.068	0.056
	%AA	61.05	66.65	70.84	81.29	80.20	82.18	61.09	63.05	66.15	70.15	76.15	80.15

*% AA= % antioxidant activity

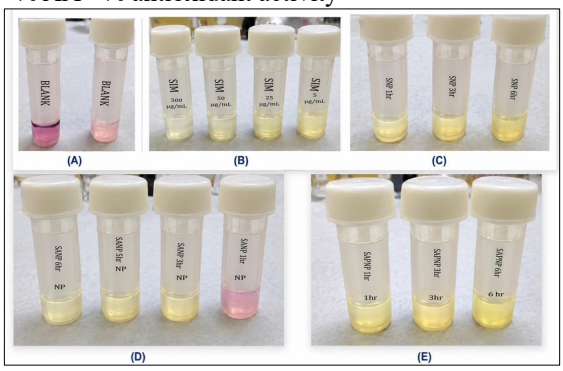

Figure 20: % DPPH activity (A) Blank reaction mixture, (B) Different formulations of Simvastatin after reaction, (C) SNP reaction mixture (D) SANP reaction mixture (E) SAPNP reaction mixture

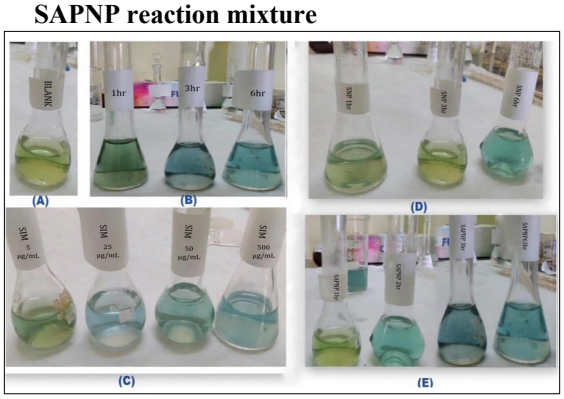

Figure 21: % NBT activity (A) Blank reaction mixture, (B) SNP reaction mixture (C) Different formulations of Simvastatin after reaction (D) SANP reaction mixture (E) SAPNP reaction mixture

In Vivo Wound Healing and Biochemical Assessment

In the STZ-induced diabetic rat wound model, SAPNP-treated animals demonstrated the highest wound-healing efficacy, achieving complete re-epithelialization within 17 days, compared with 22 days for standard treatment and 29 days for vehicle control. Biochemical analysis on days 6 and 14 showed increased total protein levels in treated groups. SAPNP and SANP treatments significantly improved antioxidant activity by increasing SOD and catalase levels. Additionally, SAPNP increased hydroxyproline and hexosamine concentrations by 41.9% and 53.9%, respectively, compared with diabetic controls, indicating enhanced collagen formation and extracellular matrix regeneration.

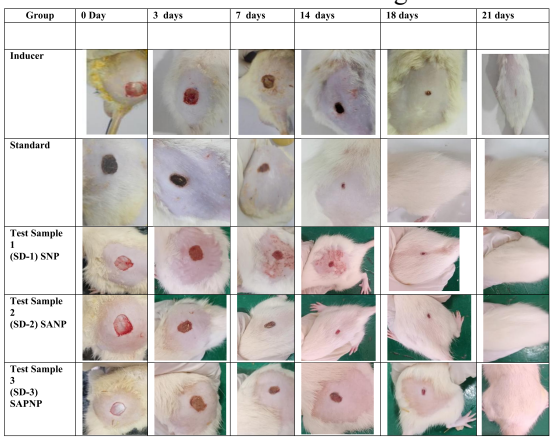

Figure 22: Animal group photographs on post-wounding days 0, 8th and 14th

Histopathological Evaluation

Histopathological examination on days 0, 8, and 14 confirmed accelerated wound healing in the SAPNP-treated group. Compared with diabetic controls showing persistent inflammation and tissue damage, SAPNP treatment promoted reduced inflammation, enhanced angiogenesis, organized collagen deposition, and complete re-epithelialization by day 14. These improvements may be attributed to the synergistic effects of simvastatin, arginine, silver nanoparticles, and PDGF in promoting tissue regeneration and cellular proliferation.

HISTOPATHOLOGY

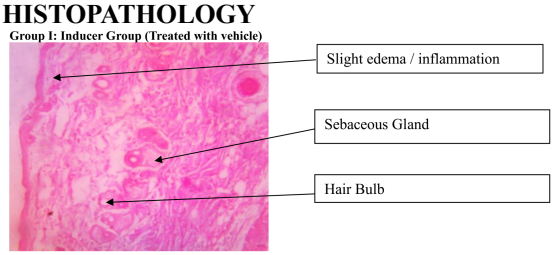

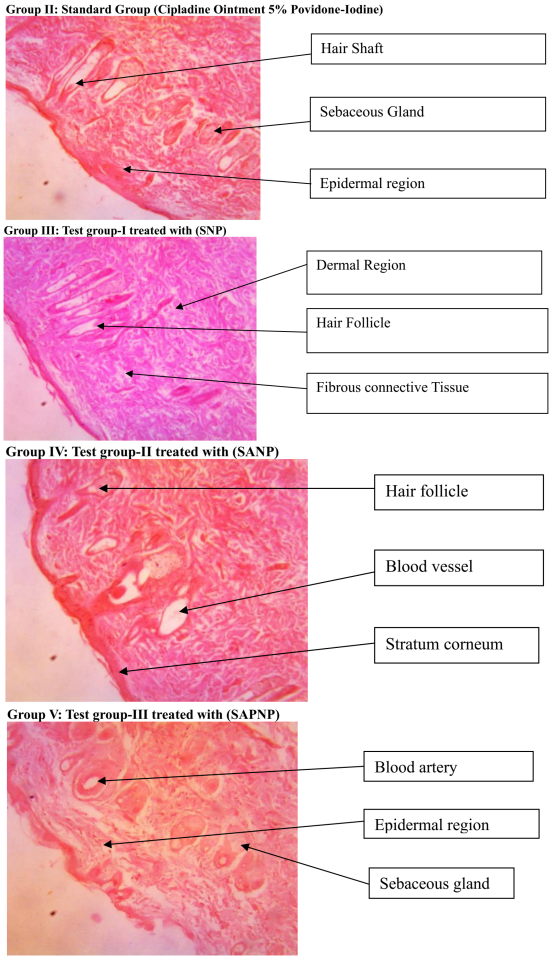

Figure 23: Histopathological section of skin on post-wounding of all animal groups

Conclusion

Diabetic wound healing is impaired by prolonged inflammation, oxidative stress, reduced growth factor levels, and delayed tissue regeneration. The present study successfully developed a multifunctional topical drug delivery system incorporating simvastatin-loaded arginine–silver nanoparticles and PDGF within a crosslinked chitosan–gelatin biopolymer ointment. The optimized nanoparticles exhibited a particle size of approximately 141.5 nm and an entrapment efficiency of 66.60%. The developed formulation demonstrated sustained drug release, antioxidant activity, antibacterial efficacy against Pseudomonas aeruginosa, and good biocompatibility. In vivo studies using STZ-induced diabetic rats demonstrated that SAPNP treatment achieved complete wound healing within 17 days. Significant improvements in SOD, catalase, total protein, hydroxyproline, and hexosamine levels further supported enhanced tissue regeneration. Histopathological findings confirmed reduced inflammation, increased angiogenesis, collagen deposition, and re-epithelialization. Overall, the developed SAPNP formulation offers a promising multifunctional approach for diabetic wound management by combining antioxidant, antimicrobial, anti-inflammatory, and tissue-regenerative properties. Further preclinical investigations and safety evaluations are required before clinical translation.

Future Perspectives

Further studies should focus on pharmacokinetic and biodistribution assessments to determine the localized retention and systemic absorption of simvastatin and PDGF. Molecular investigations using RT-qPCR and Western blotting are recommended to explore key wound-healing pathways, including PI3K/Akt/mTOR and VEGF signaling. Additionally, large-scale manufacturing, long-term stability, growth factor bioactivity, and comprehensive safety evaluations are essential to establish the clinical applicability and commercial potential of this multifunctional drug delivery system for diabetic wound management.

References

- Arana, V., Paz, Y., Gonzalez, A., Mendez, V., & Mendez, J. D. (2004). Healing of diabetic foot ulcers in L-arginine-treated patients. Biomedicine & Pharmacotherapy, 58, 588–597.
- Arginine monograph. (2005). Alternative Medicine Review, 10(2), 139-147.
- Babaei, S., Bayat, N., Nouruzian, M., & Bayat, M. (2013). Pentoxifylline improves cutaneous wound healing in streptozotocin-induced diabetic rats. European Journal of Pharmacology, 700, 165-172.
- Bagheri, M., Jahromi, B. M., Mirkhani, H., Solhjou, Z., Noorafshan, A., Zamani, A., & Amirghofran, Z. (2011). Azelnidipine, a New Calcium Channel Blocker, Promotes Skin Wound Healing in Diabetic Rats. Journal of Surgical Research, 169, e101–e107.
- Chan, Y. C., Roy, S., Khanna, S., & Sen, C. K. (2012). Downregulation of endothelial microRNA-200b supports cutaneous wound angiogenesis by desilencing GATA binding protein 2 and vascular endothelial growth factor receptor 2. Arteriosclerosis, Thrombosis, and Vascular Biology, 32, 1372-1382.
- Choi, J. K., Jang, J. H., Jang, W. H., Kim, J., Bae, I. H., Bae, J., ... & Park, J. W. (2012). The effect of epidermal growth factor (EGF) conjugated with low-molecular-weight protamine (LMWP) on wound healing of the skin. Biomaterials, 33, 8579-8590.
- Crovetti, G., Martinelli, G., Issi, M., Barone, M., Guizzardi, M., Campanati, B., ... & Carabellese, E. (2004). Platelet gel for healing cutaneous chronic wounds. Transfusion and Apheresis Science, 30, 145–151.
- Dar, A., Shafique, U., Anwar, J., Zaman, W., & Naseer, A. (2016). A simple spot test quantification method to determine formaldehyde in aqueous samples. Journal of Saudi Chemical Society, 20, S352-S356.

- Das, S., Murthy, P. N., Nath, L., & Chowdhury, P. (2010). Kinetic modeling on drug release from controlled Drug delivery systems. Acta Poloniae Pharmaceutica - Drug Research, 67, 217-223.
- Davan, S., Singer, A. J., & McClain, S. A. (2012). Persistent wound infection delays epidermal maturation and increases scarring in thermal burns. Wound Repair and Regeneration, 10, 372-377.
- Davies, P. (2003). Oral solid dosage form. In Pharmaceutical Preformulation (pp. 379-458). ISH Health Group Company, Englewood, Colorado USA.
- Eastoe, J. E. (1955). The amino acid composition of mammalian collagen and gelatin. Biochemical Journal, 61(4), 589-600.
- Escarcega-Galaz, A. A., Cruz-Mercado, J. L. D. L., et al. (2018). Chitosan treatment for skin ulcers associated with diabetes. Saudi Journal of Biological Sciences, 25(1), 130-135.
- Fernandez, A., Alvarez, A. A., Garcia, M. D., & Saenz, M. T. (2001). Anti-inflammatory effect of Pimenta racemosa var. ozua and isolation of the triterpenes lupeol. Farmaco, 56, 335-338.
- Ferreira, M. O. G., Leite, L. L. R., Lima, I. S., Barreto, H. M., Nunes, L. C. C., Ribeiro, A. B., ... & Filho, E. C. S. (2016). Chitosan Hydrogel in combination with Nerolidol for healing wounds. Carbohydrate Polymers, 152, 409-418.
- Frank, S., Hubner, G., Breier, G., Longaker, M. T., Greenhalgh, D. G., & Werner, S. (1995). Regulation of vascular endothelial growth factor expression in cultured keratinocytes. Implications for normal and impaired wound healing. Journal of Biological Chemistry, 270, 12607-12613.
- Galkowska, H., Wojewodzka, U., & Olszewski, W. L. (2006). Chemokines, cytokines, and growth factors in keratinocytes and dermal endothelial cells in the margin of chronic diabetic foot ulcers. Wound Repair and Regeneration, 14, 558–565.
- Gallo, M. B. C., & Sarachine, M. J. (2009). Biological activities of lupeol. International Journal of Biomedical and Pharmaceutical Sciences, 3(1), 46-66.
- Geetha, T., & Varalakshmi, P. (2001). Anti-inflammatory activity of lupeol and lupeol linoleate in rats. Journal of Ethnopharmacology, 76, 77–80.
- Gopal, A., Kant, V., Gopalakrishnan, A., Tandan, S. K., & Kumar, D. (2014). Chitosan-based copper nanocomposite accelerates healing in excision wound model in rats. European Journal of Pharmacology, 731, 8–19.
- Grobler, S. R., et al. (2014). Cytotoxic Effect of Chitosan-H, Resveratrol, β-Carotene and Propolis and their Chitosan Hydrogels on Balb/C Mouse 3T3 Fibroblast Cells. International Journal of Dentistry and Oral Science, 1(2), 10-14.
- Gupta, A., Upadhyay, N. K., Sawhney, R. C., & Kumar, R. (2008). A poly-herbal formulation accelerates normal and impaired diabetic wound healing. Wound Repair and Regeneration, 16, 784–790.
- Hansen, S. L., Myers, C. A., Charboneau, A., Young, D. M., & Boudreau, N. (2003). HoxD3 Accelerates Wound Healing in Diabetic Mice. American Journal of Pathology, 163, 2421–2431